

Article

Study on the Cyclic Shear Performance of Waste Steel Slag Mixed Soil

Weisheng Xu ^{1,2}, Yingna Zhu ¹, Haoran Kang ³, Qing Xu ⁴, Qipei Han ^{1,*}, Xiangwei Song ¹ and Zhenwei Liu ¹

¹ School of Civil Engineering, Architecture and Environment, Hubei University of Technology, Wuhan 430068, China; wsxu1982@whu.edu.cn (W.X.)

² School of Water Resources and Hydropower Engineering, Wuhan University, Wuhan 430072, China

³ Machinery Industry Sixth Design & Research Institute Co., Ltd., Zhengzhou 450007, China

⁴ Geological Environmental Center of Hubei Province, Wuhan 430056, China; gregoryqing@126.com

* Correspondence: 102000696@hbut.edu.cn

Abstract: Clay soil has poor engineering properties such as poor permeability and low shear strength. Waste steel slag is an industrial by-product formed in the furnace during the steelmaking process which has high quality, durability, anti-slip properties, gelling, high permeability and good particle interlocking properties. Therefore, in order to improve the engineering properties of clay and increase the utilization rate of waste steel slag, the steel slag was mixed into the clay. Steel slag clay mix was used for the straight shear test, cyclic shear test and post-cyclic straight shear test. To investigate the strength characteristics, damping ratio, shear stiffness variation and mixed soil displacement at the reinforcement-soil interface under different steel slag dosing, vertical stress, moisture content and shear amplitude conditions. The test results show that steel slag can significantly improve the shear strength of the clay tendon-soil interface, and the improvement effect is better than the conventional material sand improved clay. The steel slag mix has a large damping ratio and shear stiffness, suggesting that it has good damping and energy dissipation properties. In this case, the shear strength, damping ratio and shear stiffness of the soil mix at 40% steel slag admixture are better. The shear strength of the steel slag mix is increased after cyclic loading compared to straight shear before cyclic loading. In addition, the water content has a greater effect on the shear strength parameters, shear stiffness and damping ratio of the steel slag clay mix compared to the vertical stress and shear amplitude. The test results can provide a theoretical basis for the replacement of sand by steel slag in improving clay soils.

Keywords: cyclic shearing; damping ratio; moisture content; shear stiffness; waste steel slag



Citation: Xu, W.; Zhu, Y.; Kang, H.; Xu, Q.; Han, Q.; Song, X.; Liu, Z. Study on the Cyclic Shear Performance of Waste Steel Slag Mixed Soil. *Buildings* **2023**, *13*, 3133. <https://doi.org/10.3390/buildings13123133>

Academic Editors: Hailong Ye, Binglin Lai, Siqi Lin, Xifeng Yan and Qingfei Gao

Received: 25 March 2023

Revised: 7 December 2023

Accepted: 14 December 2023

Published: 18 December 2023



Copyright: © 2023 by the authors. Licensee MDPI, Basel, Switzerland. This article is an open access article distributed under the terms and conditions of the Creative Commons Attribution (CC BY) license (<https://creativecommons.org/licenses/by/4.0/>).

1. Introduction

China is located between the Pacific Rim and the Himalayan-Mediterranean seismic zones, and the frequency of strong earthquakes is increasing every year, damaging road foundations, retaining walls and other structures as a result [1–3]. Henri Vidal proposed the use of composite materials for the reinforcement of soil structures at the end of the 1950s. After decades of development, reinforced structures have been widely used in road foundations, retaining walls and in the prevention and control of various engineering geological hazards. Studies have shown that lateral forces such as earthquakes have a significant effect on the stability of structures such as slopes and retaining walls, and that dynamic shear modulus and damping ratio are important parameters in determining the dynamic response of soils [4]. The dynamic shear modulus reflects the bearing capacity of the soil and the damping ratio reflects the amplitude decay of the dynamic load in the soil [5]. Conventional geogrid reinforcing fill is usually sandy soil. However, sand and gravel are non-renewable resources, and the annual consumption of sand and gravel used in the construction industry alone is as much as 50 billion tons. The massive consumption has caused a growing shortage of sand and gravel materials. And with the tightening of

national environmental policies, there is a need to find new backfill materials. Li et al. [6,7] studied the feasibility of construction waste and tire chip particles as backfill material. Discarded steel slag is a by-product of steel making and is usually highly hard, resistant to water, and durable, making it a promising backfill material for application [8–11].

The highest utilization rate of steel slag in the United States, reaching 98%, of which a total utilization rate of more than 65%, is used in road construction, the current eight major railways in the United States use steel slag as railway road slag; in Germany steel slag is mainly used in construction materials and road projects, such as building foundation materials, load-bearing layer, antifreeze layer or asphalt mixture base or asphalt surface layer. China's research and use of steel slag started late after recent years of research and practice, the current use is mainly for road engineering, cement production, concrete aggregate, foundation backfill, soft ground reinforcement, etc. With regard to the practical engineering aspects of the application of waste steel slag, its mechanical properties have already been studied. Li et al. [5] studied the dynamic shear modulus and damping ratio of steel slag-sand mixes and compared them with cement-sand mixes under the same conditions. Tests have found that it is feasible to use 40% steel slag instead of 15% or less of cement mixed with sand as a foundation treatment material. Wang et al. [12] mixed steel slag into marine phase powder soil. The steel slag was used to reduce the water content of the soil and improve the bearing capacity of the foundation by taking advantage of its hard texture and strong water absorption capacity. Maghool et al. [13] investigated two major steelmaking by-products, electric arc furnace slag (EAF) and ladle furnace slag (LFS). It was found to have well gradation and strength to road engineering standards. Wang et al. [14] carried out percolation tests on steel slag with different grain sizes and clays with different steel slag contents. Liu et al. [15] prepared a new type of earth material from steel slag. It was found that the introduction of steel slag greatly improved the compressive strength and durability of the geotechnical material. Wang et al. [16] compared the mechanical properties of sand and steel slag by means of consolidation tests and direct shear tests. It was found that the mechanical properties of steel slag were similar to those of medium sand.

The study of the mechanical properties of the reinforced soil interface under cyclic loading has great significance for the practical engineering application of reinforced soils, and the interface strength index has also been an important indicator for the design of reinforced structures. At present, the shear properties of steel slag mixes under static conditions have been relatively well studied. However, less research has been carried out on the dynamic shear of steel slag mixes. Chen et al. [17] investigated the effect of the number of cyclic shears, vertical stresses, shear amplitude and other factors on the shear strength of the interlayer interface of staggered stacking soilbags. Li et al. [18] investigated the variation of shear strength parameters during cyclic shear under different vertical stress, shear amplitude and compaction conditions for domestic waste incineration subsoil-clay-polypropylene fiber mixes. Liu and Ying et al. [19,20] investigated the changes in strength properties, volume change, shear stiffness and damping ratio at the gravel-grid interface during cyclic shear. Wang et al. [21] investigated the changes in shear strength parameters at the soil-geogrid interface during cyclic and post-cyclic shear.

In this paper, a series of large-scale straight-shear and cyclic straight-shear tests were carried out. To investigate the effect of different steel slag incorporation on the cohesion, internal friction angle and vertical displacement of mixed soil under different vertical stress, moisture content and shear amplitude conditions. Analysis of the shear dynamics of the mixed steel slag reinforcement-soil interface. The results of direct shear tests on mixed soils before and after cycling were compared at the same time. We studied the effect of cyclic loading on the shear strength parameters of mixed soils. The analysis of the advantages and feasibility of steel slag as a backfill to improve clay soils.

2. Materials and Method

2.1. Materials

2.1.1. Silty Clay

The tested soil was taken from an area in Wuhan, Hubei Province, China. The raw soil was removed from impurities first, and then air dried, crushed and passed through a 2 mm sieve, after that a series of geotechnical tests were carried out in accordance with the Standard for Geotechnical Test Methods in China (GB/T50123-2019) [22]. The physical parameters of the tested soil are shown in Table 1, and this soil is classified as a typical silty clay.

Table 1. Basic physical parameter of silty clay.

Characteristics	Value
Liquid limit (%)	32.49
Plasticity index	10.6
Specific gravity	2.72
Maximum dry density (g/cm^3)	1.69
Optimum water content (%)	18.2
Cohesion (kPa)	28.44
Internal friction angle ($^\circ$)	25.08

2.1.2. Steel Slag

The steel slag is a product of a mineral processing plant in Ling Shou County. The waste steel slag selected for the test had been aged and stockpiled for more than six months and was chemically stable, as shown in Figure 1a. The XRD test analysis shows that the main components of the steel slag are calcium oxide (34.0%), silica (26.5%), magnesium oxide (12.9%), etc. The specific composition analysis is shown in Table 2. The steel slag was sieved according to the Standard for Geotechnical Test Methods in China (GB/T50123-2019) [22] and the gradation curve is shown in Figure 1b. The curvature coefficient C_C is 2.3 and the inhomogeneity coefficient C_U is 11.3. Through basic physical tests, a maximum dry density of $2.40 \text{ g}/\text{cm}^3$ and a natural water content of 7.4% were obtained for the steel slag.

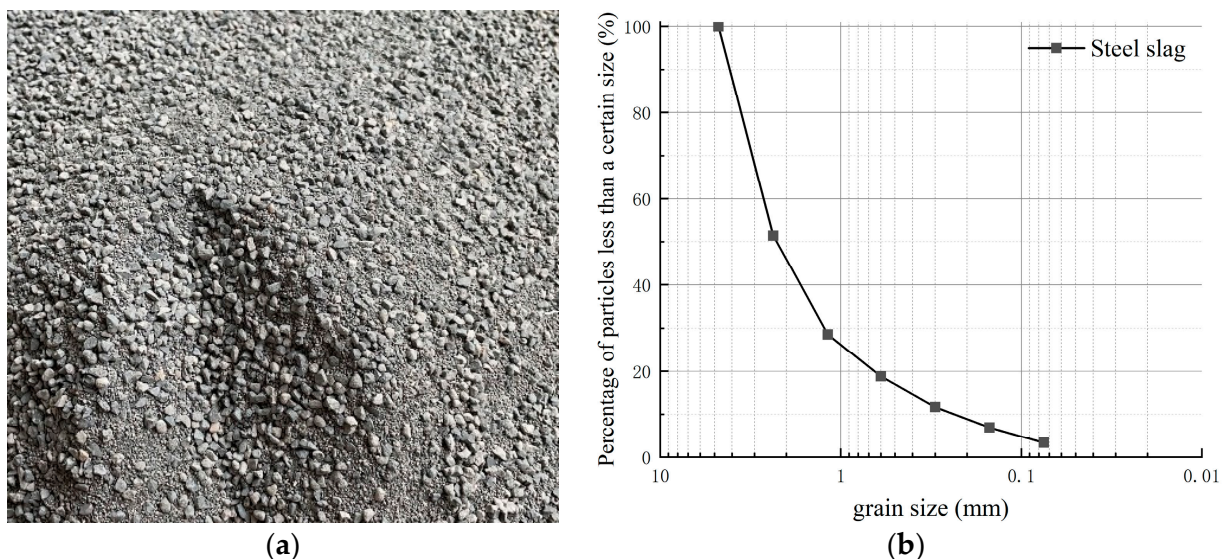


Figure 1. (a) Steel slag, (b) particle grading curve.

Table 2. Chemical composition of steel slag.

Components	Value
MgO	12.9
Al ₂ O ₃	8.7
SiO ₂	26.5
CaO	34.0
Fe ₂ O ₃	12.9
TiO ₂	0.6
MnO	1.2
Others	3.1

In this study, waste steel slag of small particle size (<5 mm) was used as the new backfill material instead of traditional sand and gravel material mixed with clay. Maghool et al. [13] carried out straight shear tests on steel slag. They found internal friction angle values in the range of 56° to 74° and cohesion-like values in the range of 99 to 121 kPa, but would exhibit significant strain softening. Because of the high self-weight of the steel slag, too high a dosing can lead to large self-weight stresses in the structure [12,13].

2.2. Method

2.2.1. Preparation of Sample

The test equipment is an XHZJ-30 large circular shear tester [19], as shown in Figure 2. The equipment consists of a shear box, upper and lower shear boxes, a support structure, five hydraulic mechanisms and their respective hydraulic power units, an electric control box and a number of internal and external sensors. The sample was 300 mm long, 300 mm wide and 300 mm high. Based on the results of the moisture-density test tests, the masses of the different proportions of mixed fill are calculated at 95% compaction. The prepared samples were covered with preservative film and left to stand for 24 h to allow for uniform moisture distribution (Figure 3). The prepared samples were filled into the assembled shear box in 6 layers (5 cm each), the height of each layer was controlled in order to control the compaction.

**Figure 2.** XHZJ-30 large circular shear tester.



Figure 3. Smothering process for Sample.

2.2.2. Shear Strength Test

The straight shear test was required according to the Chinese Standard for Geotechnical Engineering Test Methods (GB/T50123-2019) [22]. The assembly process is shown in Figure 4. The samples were tested at three different normal stresses including 200 kPa, 300 kPa, and 400 kPa and with a shear rate of 1.0 mm/min. All data are collected automatically by the acquisition system. Shear strength parameters and shear strength of mixed soils with different steel slag contents were obtained through tests. The specific test scheme is shown in Table 3.



Figure 4. Sample assembly process.

Table 3. Direct shear test scheme.

Test Types	Test Number	Sample	Vertical Stress σ /kPa	Water Content/%	Degree of Compaction
Direct shear test	T-1	30%SS + 70%C	200, 300, 400	9/12/15	95%
	T-2	40%SS + 60%C	200, 300, 400	9/12/15	
	T-3	50%SS + 50%C	200, 300, 400	9/12/15	
	T-4	C	200, 300, 400	18	

Note: steel slag (SS); clay (C); the shear rate is 1 mm/min.

2.2.3. Cyclic Shear Test

The samples were tested at three different normal stresses including 200 kPa, 300 kPa and 400 kPa at a shear rate of 1.0 mm/min. After shearing in one direction to the specified shear amplitude, the shear direction was adjusted and sheared in the reverse direction to the specified shear amplitude, and so on for 10 repetitions. The specific test scheme is shown in Table 4.

Table 4. Cyclic shear test scheme.

Test Types	Test Number	Sample	Vertical Stress σ /kPa	Shear Amplitude	Water Content/%
Cyclic shear test	T-5	30%SS + 70%C	200	5	9/12/15
	T-6	40%SS + 60%C	200/300/400	3/4/5	9/12/15
	T-7	50%SS + 50%C	300	5	9/12/15
	T-8	C	300	5	18.3

Note: The number of cycles was 10 in all cases.

The study focuses on the characteristics of the reinforcement-soil interface under cyclic shear in mixed soils with different steel slag contents. This includes the effects of normal stress, number of cycles and shear amplitude on the shear stiffness and damping ratio of the reinforcement-soil interface, and on the shear expansion and shear contraction characteristics of the sample.

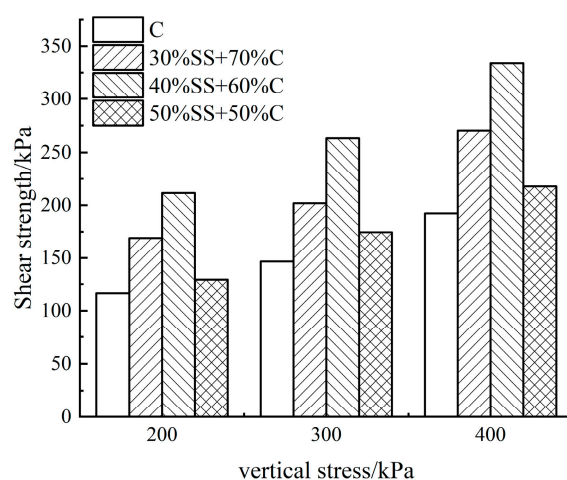
2.2.4. Shear Strength Test

The multifunctional direct shear apparatus is used for the direct shear test, which consists mainly of a mainframe and a test set-up that allows the normal stress of the apparatus to be adjusted by increasing the number of weights. The sample was prepared in a cylinder with a height of 20 mm and a diameter of 61.8 mm. The samples were tested at four different normal stresses including 100 kPa, 200 kPa, 300 kPa and 400 kPa and with a shear rate of 0.8 mm/min. All data are collected automatically by the acquisition system.

3. Results and Discussion

3.1. Shear Strength Test

The variation of shear strength with increasing steel slag content for different vertical stress conditions is shown in Figure 5. It can be seen from the graph that the shear strength of mixed soil with different steel slag content increases as the vertical stress increases. This was due to the fact that, as the vertical stress increased the denser the test, the contact area between the particles increased, leading to an increase in shear interface friction resistance, which in turn, increased the shear strength of the specimen. As the steel slag content increases, the shear strength of the soil mix tends to increase and then decrease. For instance, the shear strength of the soil under 300 kPa vertical stress is 159 kPa for clay, 201 kPa for 30% steel slag mix, 263 kPa for 40% steel slag mix and 174 kPa for 50% steel slag mix.

**Figure 5.** Shear strength of different steel slag content.

The relationship between shear stress and shear displacement for specimens with different moisture contents is shown in Figure 6. From Figure 6a, it was found that: the shear resistance of the specimens at 9% moisture content is optimal when the steel slag is mixed at 30%. From Figure 6b, it was found that: the shear resistance is optimal at 12% moisture content specimens when the steel slag is mixed at 40%. Peak shear strength at 18% moisture content decreased by 67.6% compared to 12% moisture content. This indicates that samples with higher moisture content are more plastic, and therefore, only three moisture contents of 9%, 12% and 15% will be considered in subsequent tests. From Figure 6c, it was found that: the shear resistance of the specimen was optimal at 12% moisture content when the steel slag was mixed with 50%, and at 15% moisture content, the shear stress increased and then decreased with shear displacement, showing an obvious strain softening phenomenon.

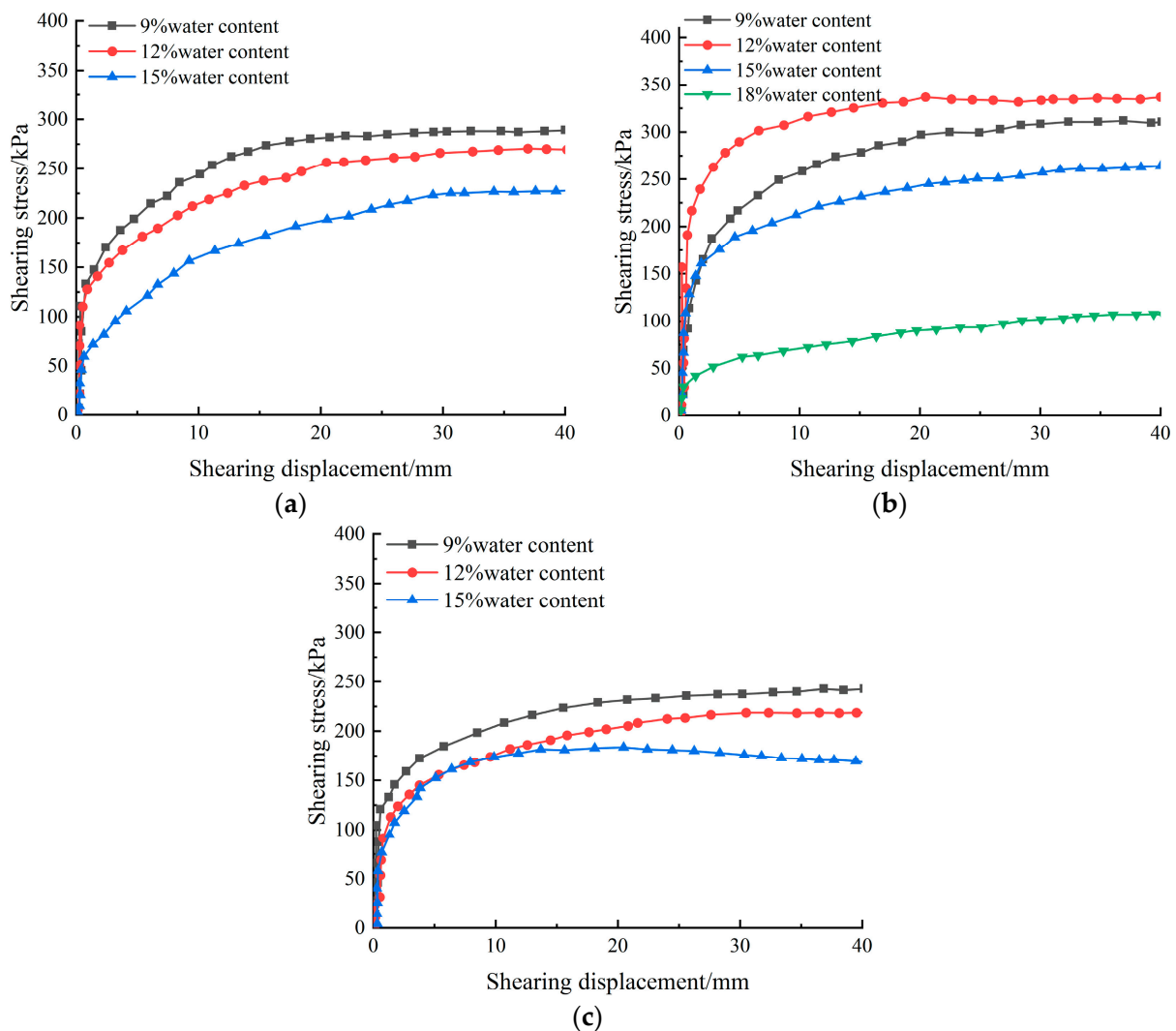


Figure 6. Shear stress-shear displacement relationship curves at different moisture contents (a) 30%SS + 70%C; (b) 40%SS + 60%C; (c) 50%SS + 50%C.

Table 5 shows that the cohesion of the soil mix decreases with the increase in the amount of steel slag, but increases compared to clay, and the angle of internal friction increases slightly. This phenomenon was caused by the incorporation of steel slag, which took up the space for the clay particles to bind, thus reducing the degree of adhesion and cohesion of the soil. It was shown by Maghool et al. [13] that steel slag particles themselves

have a high internal friction angle, so the incorporation of steel slag can effectively increase the friction angle within the soil.

Table 5. Comparison of cohesion and internal friction angle of different materials.

Sample	c/(kPa)	$\varphi/(^{\circ})$
30%SS + 70%C	92.62	26.86
40%SS + 60%C	87.74	32.10
50%SS + 50%C	43.31	30.17
C	34.64	23.83

As can be seen from Table 6, as the water content increases, both the cohesion and the angle of internal friction of the soil decrease. When the moisture content increases by 6%, the cohesion of the soil is reduced by 56% with 30% steel slag, by 22% with 40% steel slag and by 42% with 50% steel slag. Causes of reduced cohesion and angle of internal friction. It may be that when the water content is high, the water in the soil acts mainly as a lubricant. Because of the water film, large agglomerates are formed between the particles. This resulted in a reduction in the correlation between soil particles.

Table 6. Comparison of cohesion and internal friction angle with different water content.

Sample	Water Content/%	c/(kPa)	$\varphi/(^{\circ})$
30%SS + 70%C	9%	117.81	27.97
	12%	92.62	26.86
	15%	51.33	24.89
40%SS + 60%C	9%	108.66	27.33
	12%	87.74	32.10
	15%	85.16	25.69
50%SS + 50%C	9%	67.12	30.17
	12%	43.31	24.10
	15%	39.47	19.62

The above comparative analysis found that: The incorporation of steel slag can effectively increase the cohesion and internal friction angle of the clay. The mix with 40% steel slag incorporation has a greater cohesion and angle of internal friction than the excellent backfill (sand-clay mix) derived from previous studies. It shows that steel slag can be used as an improved material instead of sand.

3.2. Cyclic Shear Test

3.2.1. Cycle Load Effect on Shear Strength

The curve of the peak shear stress of the soil mix with the number of cycles for different levels of steel slag incorporation is shown in Figure 7. As shown in the Figure, the peak shear stress of the soil mix increases significantly with the number of cycles after the steel slag is incorporated into the clay. This was due to the gradual densification of the soil particles by rearrangement during the circulation process. Compared to mixed soils, pure clay has a lower peak shear stress and a significantly lower growth rate. The shear strengths of the 30%, 40% and 50% steel slag mixes were 8.7%, 16% and 13.1% higher, respectively, than the clay. It showed that the steel slag was effective in improving the shear strength of the clay.

The curve of the shear stress of 40% steel slag mix, with the number of cycles under different shear amplitude conditions, is shown in Figure 8. The graph shows that as the shear amplitude increases, the peak shear stress increases. Compared to the first cycle, after 10 cycles, the incremental peak shear stress was 81.7% at $A = 3$ mm, 84.9% at $A = 4$ mm and 100.6% at $A = 5$ mm. This is because the higher the shear amplitude the more compact the alignment of the soil particles at the reinforced soil interface, resulting in a higher shear strength.

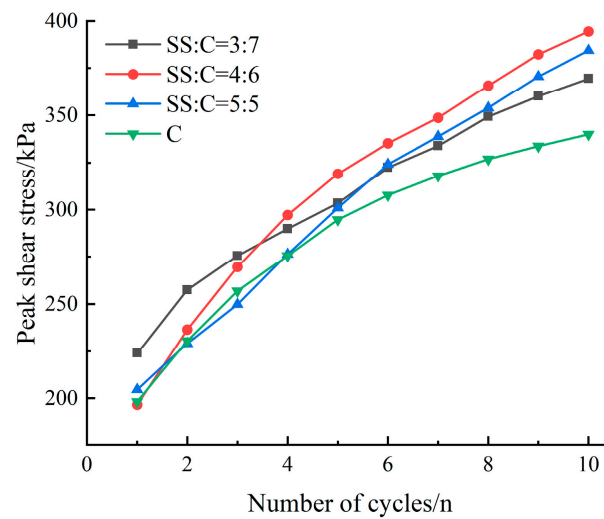


Figure 7. Mixed soil reinforced soil interface cycle number-shear stress peak relationship curve.

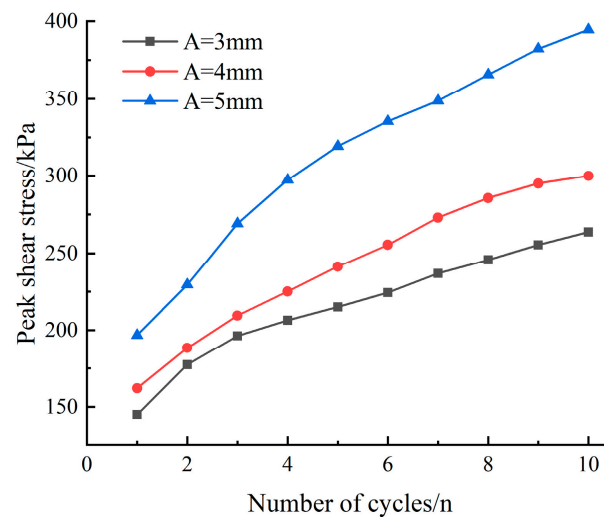


Figure 8. The relationship curve between the number of cycles and the peak shear stress of the reinforced soil interface with different shear amplitudes.

The variation in shear stress with the number of cycles for a 40% steel slag inclusion mix at different moisture contents is shown in Figure 9. It was found that the peak shear stress of the steel slag mix gradually decreased with increasing water content and remained essentially the same around the optimum water content. The peak shear stress decreases significantly at high moisture content conditions. The shear stress remains essentially constant with an increasing number of cycles. The shear strength of the soil mix decreases by 1.4% to 8.5% when the water content is increased from 9% to 12% and by 47.6% to 58.6% when the water content is increased from 12% to 15%. This is probably due to the fact that under high water content conditions, part of the water is present in the soil as free water to act as a lubricant, weakening the friction between the soil particles.

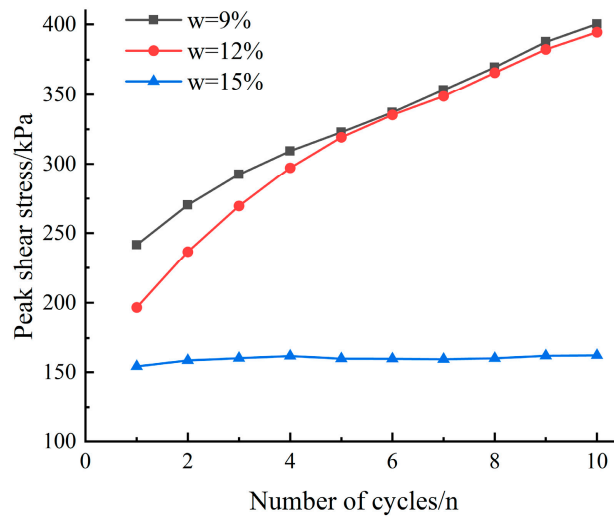


Figure 9. Moisture content to peak shear stress curve.

3.2.2. Shear Stiffness and Damping Ratio

The shear stiffness and damping ratio of the soil were the two main parameters to be considered in the dynamic design of soil structures. Desai, Nye and Liu Fei yu et al. [23–26] modified the stiffness damping ratio approach and used it to describe the dynamic response analysis of the sand-concrete interface, as shown schematically in Figure 10. Based on the shear stress and shear strain at the vertices of the hysteresis loop model. Consider the asymmetry of the hysteresis loop in both shear directions. The shear stiffness K is determined according to Equation (1) and the damping ratio D is determined according to Equation (2).

$$K = \frac{K_1 + K_2}{2} = \frac{\tau_1 + \tau_2}{2A} \tag{1}$$

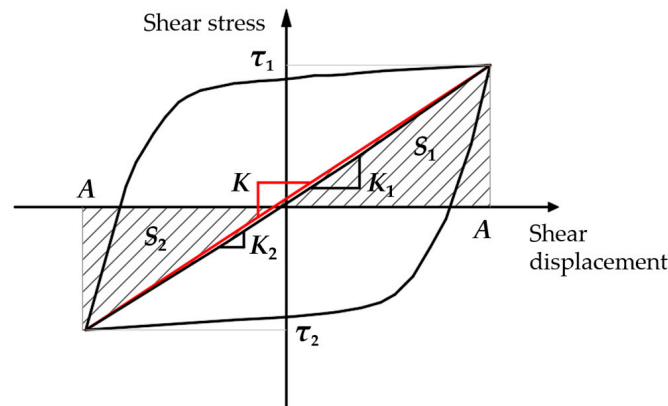


Figure 10. Schematic diagram of shear stiffness and damping ratio calculation.

K_1, K_2 is the shear stiffness in both shear directions, τ_1, τ_2 is the peak shear stress in both shear directions, A is the shear displacement amplitude.

$$D = \frac{D_1 + D_2}{2} = \frac{1}{2} \left(\frac{S}{4\pi S_1} + \frac{S}{4\pi S_2} \right) = \frac{S}{4\pi A} \left(\frac{1}{\tau_1} + \frac{1}{\tau_2} \right) \tag{2}$$

D_1, D_2 is the damping ratio in both shear directions, S_1, S_2 is the area of the shaded portion in Figure 2, and S is the area of the entire hysteresis loop.

The shear stiffness of the soil mixture of different materials with the number of cycles when subjected to 300 kPa vertical stress is shown in Figure 11a. It can be seen that the

shear stiffness of the mixed soil increases with the number of cycles due to the low contact between the particles and the shear interface in the initial stage [25]. As the number of cycles increases, the particles at the interface rearrange so that the contact becomes larger, leading to an increase in the stiffness of the interface. For the first cycle, the 30%, 40% and 50% steel slag dosing corresponded to shear stiffnesses of 46.4 MPa/m, 40.8 MPa/m and 37.7 MPa/m, and the clay corresponded to a shear stiffness of 41.4 MPa/m. The more slag is incorporated the lower the initial stage shear stiffness. This was due to the larger steel slag particles and the increased admixture resulting in less contact between the particles and the interface, so the initial stage shear stiffness was less. Figure 11b shows the variation of the damping ratio with the number of cycles for different material mixes when subjected to 300 kPa vertical stress. The damping ratio increases with the amount of steel slag incorporated, and both weaken with the increase in the number of cycles and then stabilize. The damping ratio of one of the mixes with a high steel slag content decreases significantly after the first cycle. This was due to the high number of pores between the particles in the initial state, but the decrease in pores and the increase in force transfer paths led to a significant decrease in the damping ratio during shear due to the low strength of the particles, which led to their fragmentation [27,28].

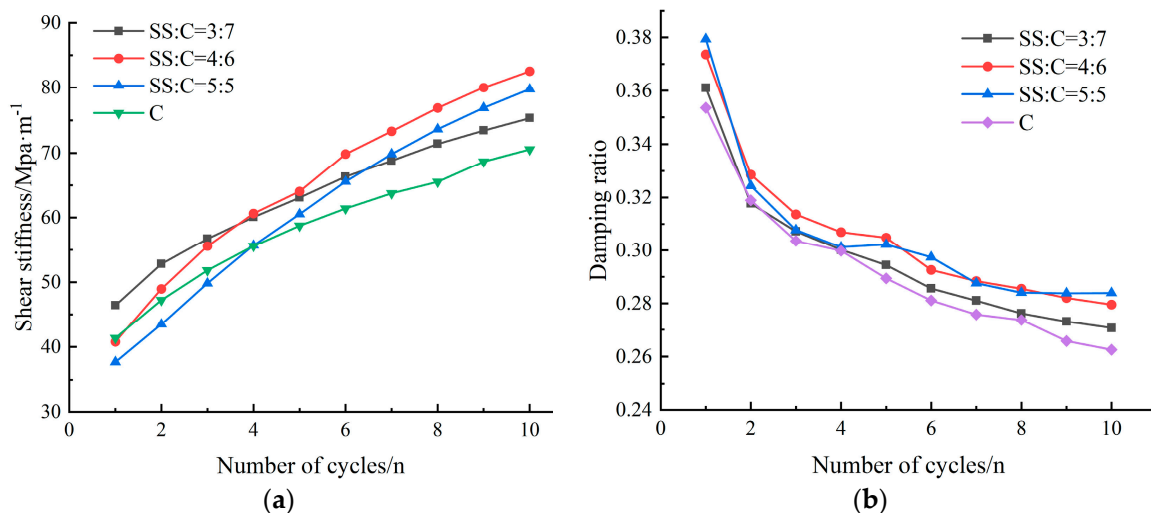


Figure 11. Shear stiffness and damping ratio of soil mixtures of different materials (a) shear stiffness; (b) damping ratio.

The shear stiffness of the mixed soil after 40% steel slag incorporation with the number of cycles at different moisture contents under 300 kPa vertical stress is shown in Figure 12a. It was found that the mixed soil shear stiffness decreases with increasing water content. At 9% and 12% moisture content, the shear stiffness increases with the number of cycles, while at 15% moisture content, the shear stiffness remains essentially constant with the number of cycles. It may be that some free water exists within the soil pores and that excess water cannot be drained in time during cyclic shearing. The dynamic pore water pressure is formed, which reduces the soil's ability to resist deformation, so the shear stiffness is less [27]. Figure 12b shows the variation curve of the damping ratio with the number of cycles of the mixed soil after 40% steel slag incorporation at different moisture contents under 300 kPa vertical stress. It was found that the damping ratio of the mixed soil increases with increasing water content and weakens with an increasing number of cycles before it stabilizes. This was due to the increase in free inter-pore water between the particles as the water content increased. These pore waters dissipate energy as the pore pressure changes movement during cyclic shear, so the damping ratio increases with increasing water content. As the number of cycles increases, the contact between particles becomes closer, the force

transfer pathway increases and the energy consumption in vibration decreases, so the damping ratio decreases with the number of cycles [28].

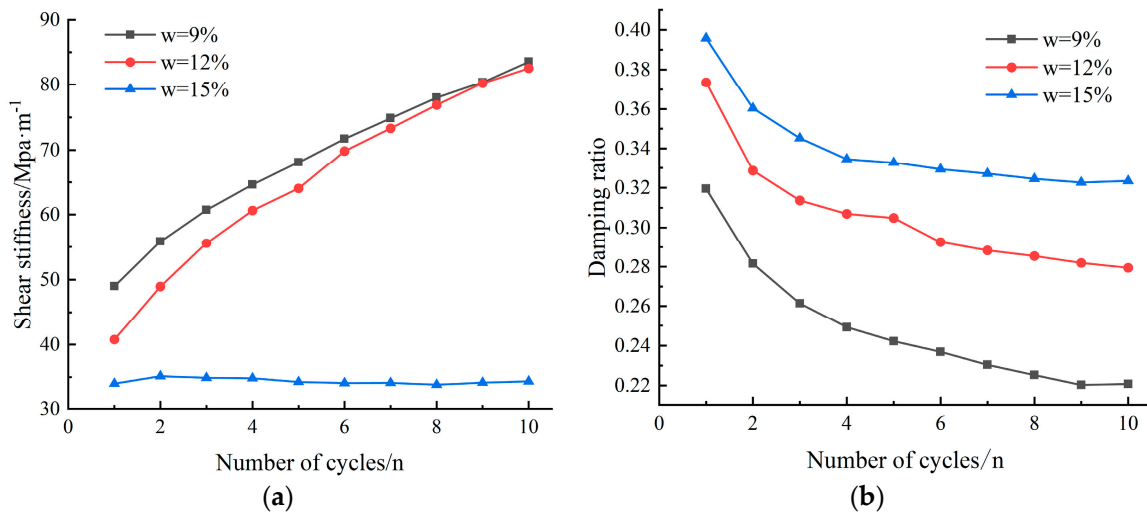


Figure 12. Shear stiffness and damping ratios at different moisture contents of 40% steel slag mixes (a) shear stiffness; (b) damping ratio.

The variation in shear stiffness with the number of cycles for different shear amplitudes of 40% steel slag incorporated into the soil mix at 300 kPa vertical stress is shown in Figure 13a. It was found that the mixed soil shear stiffness decreases with increasing shear amplitude and increases with the number of cycles, but the growth rate gradually decreases. Figure 13b shows the variation curve of the damping ratio of 40% steel slag blended soil with the number of cycles at different shear amplitudes under 300 kPa vertical stress. As can be seen: the damping ratio of mixed soil decreases with increasing shear amplitude, decreases with increasing number of cycles, and the rate of decrease gradually decreases. For the first cycle, shear amplitudes of 3 mm, 4 mm and 5 mm correspond to damping ratios of 0.43, 0.38 and 0.37. The reductions after 10 cycles were 23.3%, 23.7% and 24.3%, respectively. It was suggested that the incorporation of steel slag gives the mix a better energy dissipation capacity at smaller strains and as a backfill material can absorb more energy in small earthquakes [17,28].

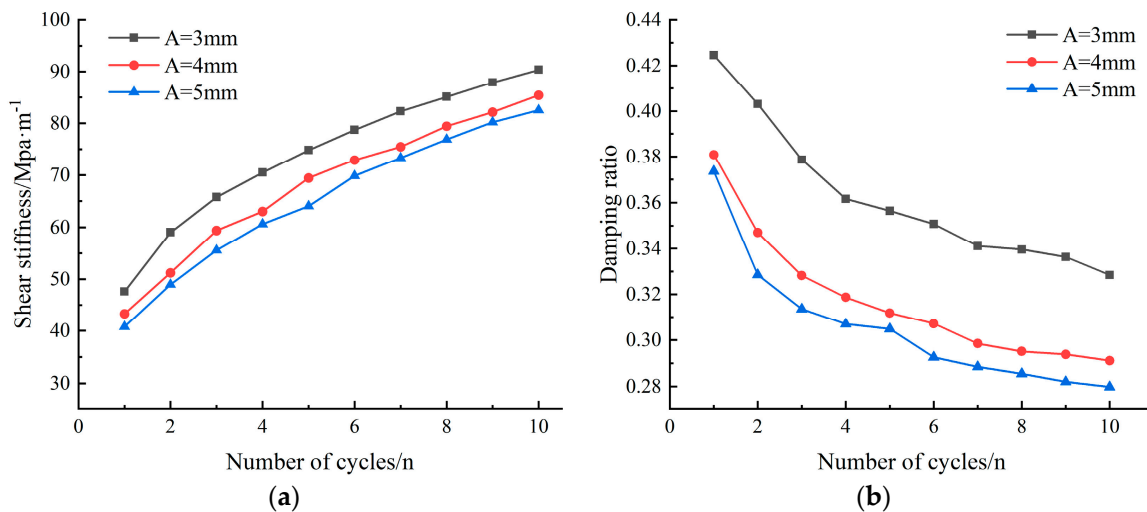


Figure 13. Shear stiffness and damping ratio of 40% steel slag mixed soil with different shear amplitudes (a) shear stiffness; (b) damping ratio.

3.2.3. Vertical Displacement under Cyclic Load

As the shear surface area remains constant during shear, the volume change can be represented by the vertical displacement. Figure 14 shows the curves of vertical displacement and horizontal displacement of mixed soils of different materials at 300 kPa. Positive values of vertical displacement indicate volume contraction [19]. The volume contraction phenomenon in the graph was mainly attributed to the compaction of the pores between the particles. The different material mixes all show a more significant increase in vertical displacement in the first cycle and a decreasing trend in the increase of vertical displacement with an increasing number of cycles. The corresponding final vertical displacements were 16.1 mm, 15.8 mm and 17.4 mm at 30%, 40% and 50% of the steel slag admixture. The clay corresponds to a final vertical displacement of 23.0 mm. It was shown that the incorporation of steel slag was effective in reducing the bulk change of the clay for the same shear area.

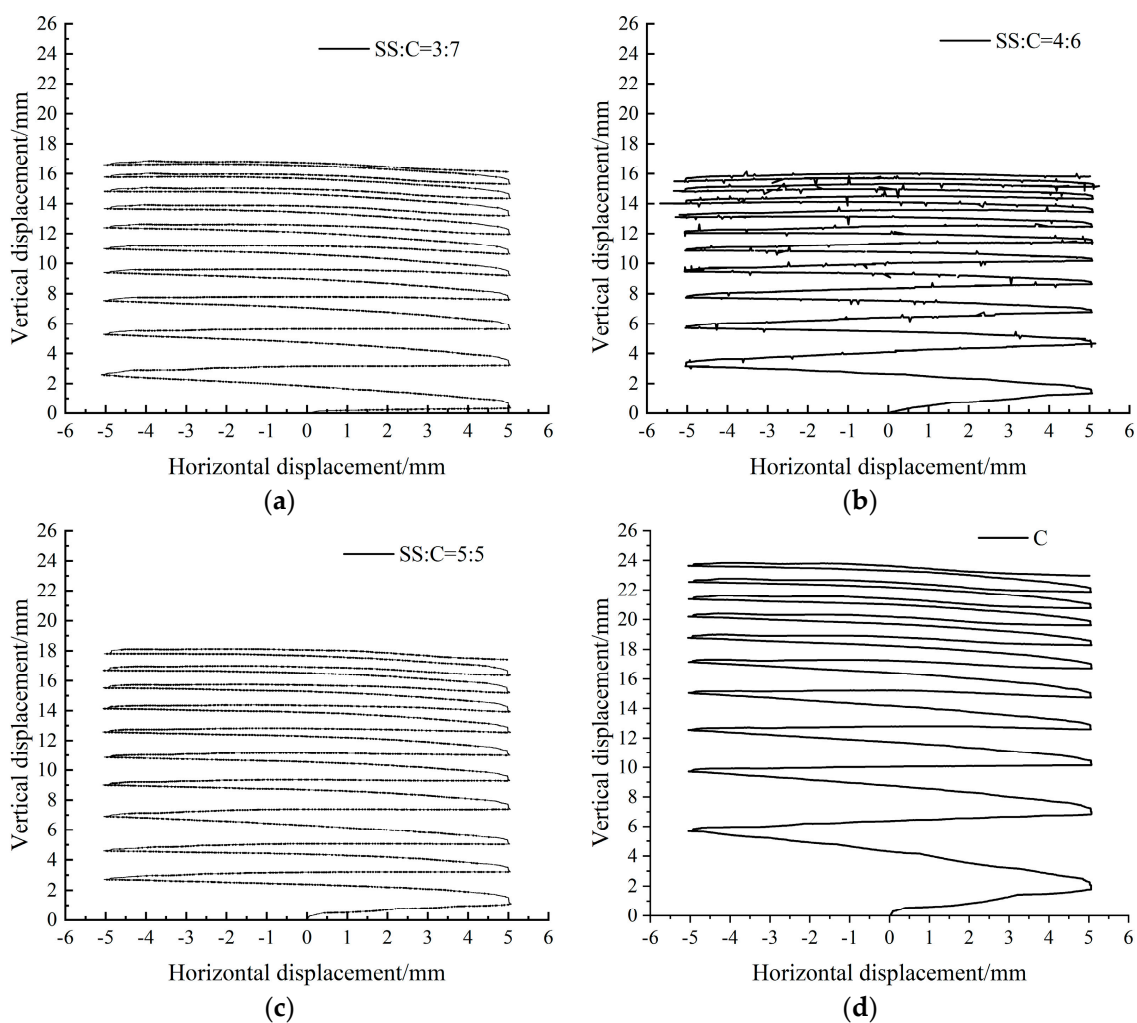


Figure 14. Horizontal displacement-verticall displacement variation curves for mixed soils of different materials (a) SS:C = 3:7; (b) SS:C = 4:6; (c) SS:C = 5:5; (d) C.

The variation curves of vertical displacement and horizontal displacement of mixed soils with different moisture contents for a steel slag content of 40% are shown in Figure 15. It was found that the vertical displacement increases with increasing water content, and the change in vertical displacement was more significant in the first cycle. The final vertical displacements corresponding to 9%, 12% and 15% moisture content were 12.8 mm, 15.8 mm and 18.2 mm, corresponding to vertical displacement increments of 3.1 mm, 4.6 mm and

7.6 mm for the first cycle. This was due to the fact that, with higher water content soils, the surface of the soil grains had a thickened film of bound water. The viscosity of the water was reduced, dissolving between the cementing substances in the soil and reducing the cohesion. This resulted in a reduced interaction between the particles [28].

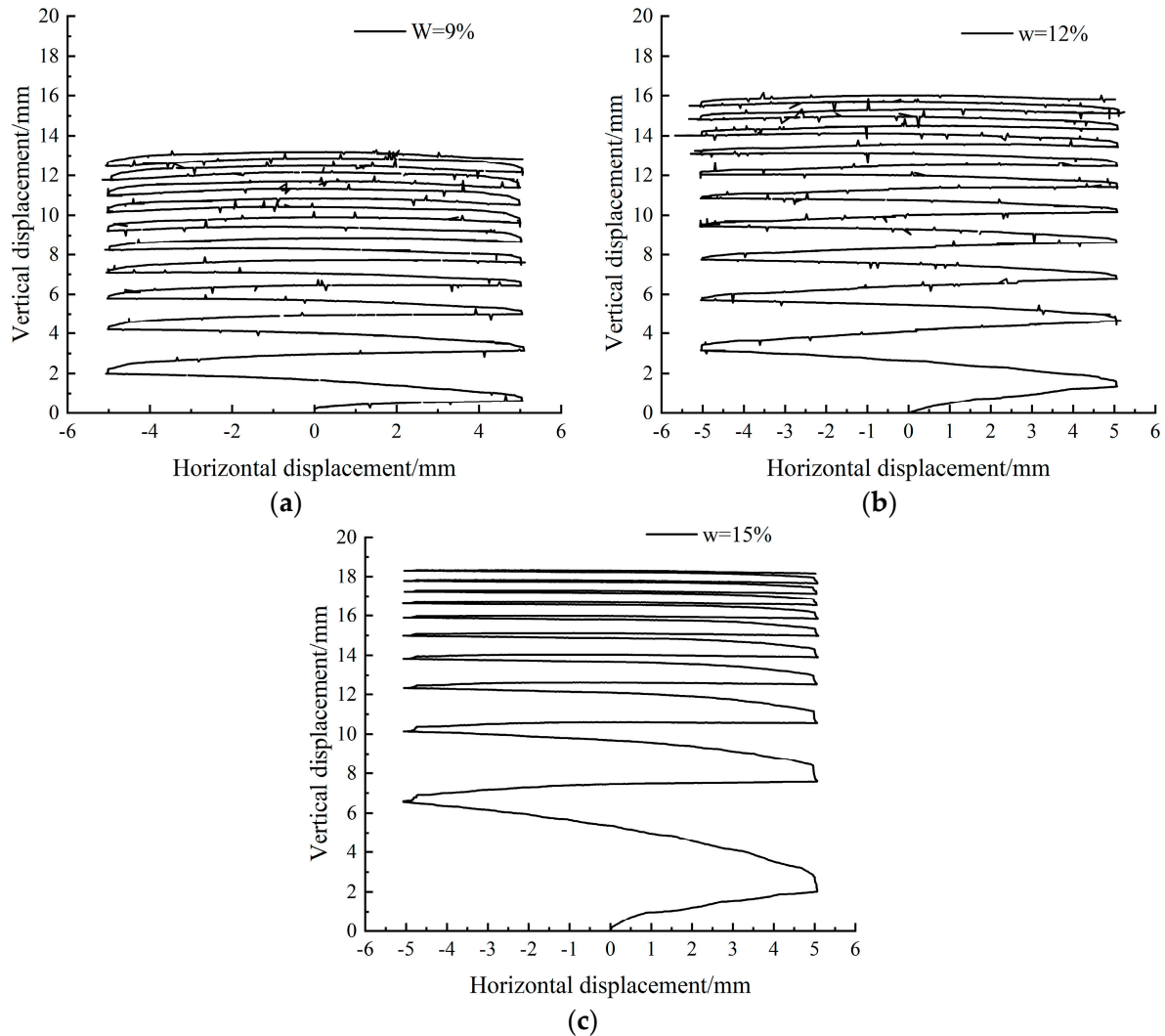


Figure 15. Horizontal displacement-vertical displacement variation curves for different moisture contents of 40% steel slag mix (a) 9%; (b) 12%; (c) 15%. (a) Cohesion and (b) Internal friction angle.

3.3. Post-Cycle Shear Test Disintegration Rate

Controlled shear amplitude of 5 mm and steel slag dosing of 40% were used for post-cycle straight shear tests. Figure 16 shows the shear stress-displacement relationship curves for different vertical stress conditions. From Figure 16a it was found that at 200 kPa, 300 kPa and 400 kPa vertical stress conditions, compared to the pre-circulation mixed soil interface shear strength, the post-circulation mixed soil interface shear strength increased significantly, by 12.8%, 37.4% and 56.1%, respectively. This was because after experiencing cyclic shear, the soil compactness at the interface was further increased, so the reinforcing material restrained the steel slag mix more fully, and the increase of the interface compactness made the frictional occlusion at the interface intensified, resulting in a larger shear strength of the soil after experiencing cyclic shear. The shear displacement corresponding to the smooth point of shear strength at the interface is shifted back. As shown in Figure 16b, the interfacial shear strength of the mixed soil increased significantly after circulation at

9% and 12% water content, with increases of 79.0% and 56.1%, respectively. The interfacial shear strength of the soil mix at 15% moisture content was slightly reduced by 11.7%. This was caused by the fact that when the water content is high, the higher amount of water on the one hand acts as a lubricant within the soil and reduces the cohesion and friction between particles; on the other hand, there might be some free water within the pores of the soil. During cyclic loading, a certain dynamic pore water pressure was developed, which reduced the effective stress. As a result, the shear strength of the mixed soil interface is reduced at higher water contents.

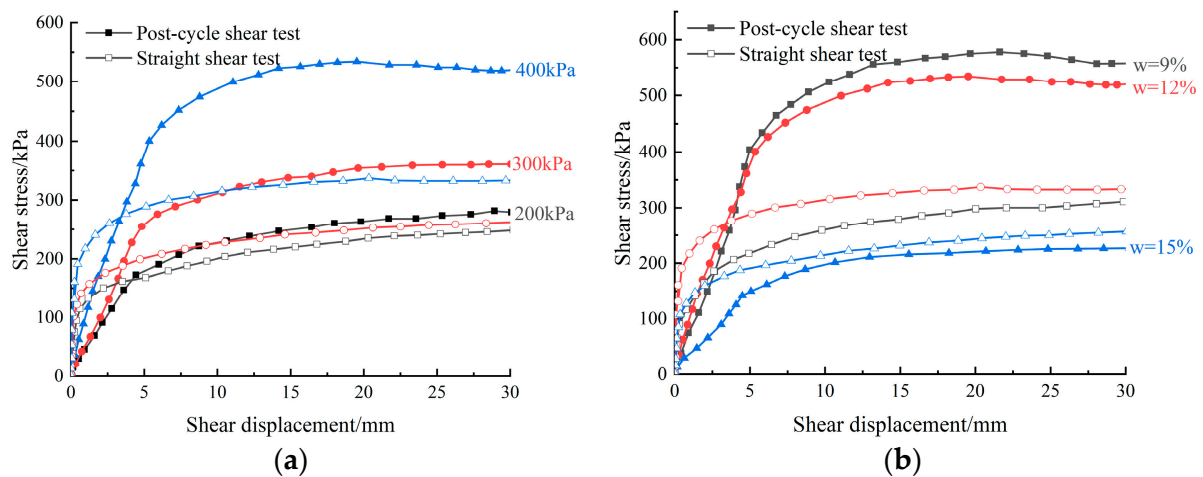


Figure 16. Shear stress-shear displacement relationship before and after cyclic shear. (a) under different vertical stress conditions, (b) under different moisture content conditions.

The shear strength envelope curves of the mixed soil interface for the straight shear test and the post-cycle straight shear test are shown in Figure 17. By linear fitting, the soil shear strength parameters for the pre- and post-cycle direct shear tests were obtained as shown in Table 7. After the cyclic shear, it can be seen that the cohesion at the soil interface increases slightly and the angle of internal friction also increases.

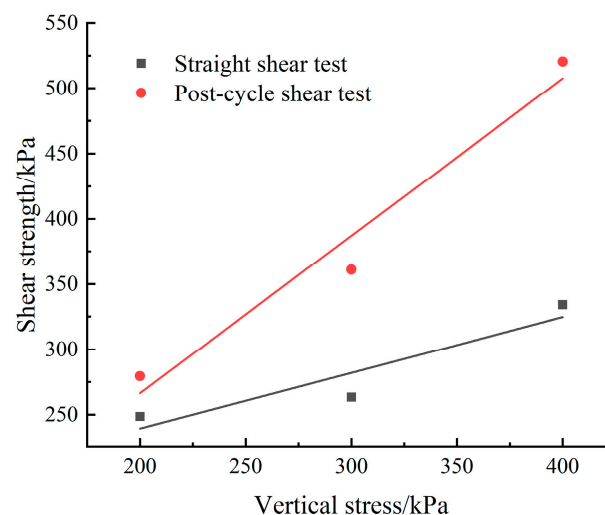


Figure 17. Interface shear strength envelope curves.

Table 7. c , φ values of straight shear test, straight shear test after circulation.

Test Type	c/kPa	$\varphi/^\circ$
Straight shear test	87.7	32.1
Post-cycle shear test	95.4	50.3

4. Conclusions

This study presents straight shear tests, cyclic shear tests and post-cyclic shear tests on steel slag mixes. We investigated the shear strength characteristics and cyclic shear properties of mixed soils under different vertical stress, shear amplitude and moisture content conditions. The main conclusions obtained are as follows:

- (1) Steel slag incorporation improves the shear strength of the soil interface and increases the cohesion and angle of internal friction of the soil mix. Vertical displacement decreased. The cohesion of the soil mix decreases with increasing steel slag content and the angle of internal friction increases. The shear strength of the soil interface decreases as the water content increases and the mechanical parameters of shear strength all decrease.
- (2) In cyclic shear tests, under different vertical stress, shear amplitude and moisture content conditions, it was found that:
 - (a) The mixed soils all showed cyclic shear hardening and shear shrinkage. The shear reduction decreases as the number of cycles increases. At high water content conditions, the peak shear stress at the interface of the mixed soil remains essentially constant with an increasing number of cycles.
 - (b) As the shear amplitude increases, the shear stiffness to damping ratio of the soil interface decreases. As the number of cycles increases, the shear stiffness of the soil interface increases and the damping ratio decreases.
 - (c) A decrease in soil interface shear stiffness and an increase in damping ratio with increasing water content and an increase in the number of cycles increased shear stiffness and reduced damping ratio at the soil interface. Shear stiffness remained stable with an increasing number of cycles at 15% moisture content.
- (3) Compared to the results of the direct shear test, there was a significant increase in shear strength, a slight increase in cohesion and a significant increase in the angle of internal friction in the post-cycle direct shear test soil mix.
- (4) The shear resistance of the 40% steel slag mix was superior. Under cyclic shear loading, better damping and energy dissipation can be demonstrated. For reference when selecting ratios for practical engineering applications.

A 40% steel slag content was found to be the best choice for dealing with the problem of low shear strength in clayey soils. The investigation showed that clay can be mixed with steel slag for light traffic roads and some retaining structures. In this study, indoor mechanical tests were conducted only on steel slag mixed clay, a new type of filler. Subsequent indoor scale-down model tests or in-situ tests will be conducted to further validate this new backfill application.

Author Contributions: Conceptualization, W.X.; Validation, Z.L.; Investigation, H.K.; Resources, Q.X.; Writing—original draft, H.K.; Writing—review & editing, Y.Z.; Visualization, Y.Z. and X.S.; Supervision, Q.X. and Q.H.; Project administration, Q.H.; Funding acquisition, W.X. All authors have read and agreed to the published version of the manuscript.

Funding: The authors are thankful for the financial support from the National Natural Science Foundation of China (No. 52278347, 52208339), the Key Research and Development Program of Hubei Province (2022BCA059), the Joint Funds of the National Nature Science Foundation of China (No. U22A20232) and Hubei University of Technology Outstanding Talent Fund Project (XJ2021000501).

Data Availability Statement: The data provided in this study are available upon request from the corresponding author. Due to data confidentiality, these data are not available to the public.

Conflicts of Interest: Author Haoran Kang was employed by the company Machinery Industry Sixth Design & Research Institute Co., Ltd. The remaining authors declare that the research was conducted in the absence of any commercial or financial relationships that could be construed as a potential conflict of interest.

References

1. Shou, K.J.; Hong, C.Y.; Wu, C.C.; Hsu, H.Y.; Fei, L.Y.; Lee, J.F.; Wei, C.Y. Spatial and temporal analysis of landslides in Central Taiwan after 1999 Chi-Chi earthquake. *Eng. Geol.* **2011**, *123*, 122–128. [[CrossRef](#)]
2. Huang, R.; Pei, X.; Fan, X.; Zhang, W.; Li, S.; Li, B. The characteristics and failure mechanism of the largest landslide triggered by the Wenchuan earthquake, May 12, 2008, China. *Landslides* **2012**, *9*, 131–142. [[CrossRef](#)]
3. Yin, Y.; Wang, F.; Sun, P. Landslide hazards triggered by the 2008 Wenchuan earthquake, Sichuan, China. *Landslides* **2009**, *6*, 139–152. [[CrossRef](#)]
4. Kumar, J.; Madhusudhan, B.N. Dynamic properties of sand from dry to fully saturated states. *Geotechnique* **2012**, *62*, 45–54. [[CrossRef](#)]
5. Li, W.; Lang, L.; Wang, D.; Wu, Y.; Li, F. Investigation on the dynamic shear modulus and damping ratio of steel slag sand mixtures. *Constr. Build. Mater.* **2018**, *162*, 170–180. [[CrossRef](#)]
6. Li, L.-h.; Wen, B.; Hu, Z. Study on reinforced shear behavior of construction waste filler and geosynthetics. *J. Wuhan Univ.* **2019**, *52*, 311–316.
7. Li, L.-h.; Xiao, H.-l.; Tang, M.-h.; Hu, Q.Z.; Sun, M.J.; Sun, L. Dynamic properties variation of tire shred-soil mixtures. *Rock Soil Mech.* **2014**, *35*, 359–364, 422.
8. Dang, D.T.; Nguyen, M.T.; Nguyen, T.P.; Isawa, T.; Ta, Y.; Sato, R. Mechanical properties of steel slag replaced mineral aggregate for road base/sub-base application based Vietnam and Japan standard. *Environ. Sci. Pollut. Res.* **2022**, *29*, 42067–42073. [[CrossRef](#)]
9. Vashistha, P.; Park, S.; Pyo, S. A Review on Sustainable Fabrication of Futuristic Cementitious Binders Based on Application of Waste Concrete Powder, Steel Slags, and Coal Bottom Ash. *Int. J. Concr. Struct. Mater.* **2022**, *16*, 51. [[CrossRef](#)]
10. Wang, C.; Zhang, C. Deformation of Steel Slag Asphalt Mixtures Under Normal Temperature Water Immersion. *Front. Mater.* **2021**, *8*, 718516. [[CrossRef](#)]
11. Jiao, W.; Sha, A.; Liu, Z.; Li, W.; Jiang, W.; Qin, W.; Hu, Y. Study on thermal properties of steel slag asphalt concrete for snow-melting pavement. *J. Clean. Prod.* **2020**, *277*, 123574. [[CrossRef](#)]
12. Wang, L.-y.; Zhang, B.; Xie, H.; Ji, W.; Huang, X. Study on Shear Strength Characteristics of Marine Silt Modified by Steel Slag. *Adv. Civ. Eng.* **2021**, *2021*, 9647977. [[CrossRef](#)]
13. Maghool, F.; Arulrajah, A.; Suksiripattanapong, C.; Horpibulsuk, S.; Mohajerani, A. Geotechnical properties of steel slag aggregates: Shear strength and stiffness. *Soils Found.* **2019**, *59*, 1591–1601. [[CrossRef](#)]
14. Wang, L.; Yan, J.; Wang, Q.; Wang, B.; Ishimwe, A. Study on Permeability of Steel Slag and Steel Slag Modifying Silt Soil As New Geo-backfill Materials. *J. Eng.* **2019**, *2019*, 5370748. [[CrossRef](#)]
15. Liu, X.; Hu, M.; Ke, S.; Fu, C.; Guo, X.; Ye, X. A novel rammed earthen material stabilized with steel slags. *Constr. Build. Mater.* **2018**, *189*, 1134–1139. [[CrossRef](#)]
16. Wang, L.Y.; Wang, Q.; Huang, X.; Yan, J. Experimental Investigation on Compressive Deformation and Shear Strength Characteristics of Steel Slag in the Geotechnical Engineering. In Proceedings of the Geoshanghai International Conference, Shanghai, China, 27–30 May 2018; Springer: Singapore, 2018.
17. Chen, S.; Jia, F.; Liu, S.; Li, J. Experiments on the cyclic shear behavior of the interface between staggered stacking soilbags. *Chin. J. Rock Mech. Eng.* **2021**, *40*, 2945–2953.
18. Liu, F.-y.; Jiang, H.; Wang, J. Experimental study on cyclic shear softening characteristics of gravel-geogrid interface. *Rock Soil Mech.* **2021**, *42*, 1485–1492.
19. Li, L.-h.; Zang, T.-b.; Liu, Y.-l. Cyclic shear performance of fiber bottom ash mixed soils. *Chin. J. Rock Mech. Eng.* **2021**, *40*, 196–205.
20. Ying, M.-j.; Wang, J.; Liu, F.Y.; Li, J.T.; Chen, S.Q. Analysis of cyclic shear characteristics of reinforced soil interfaces under cyclic loading and unloading. *Geotext. Geomembr.* **2022**, *50*, 99–115. [[CrossRef](#)]
21. Wang, J.; Liu, F.Y.; Wang, P.; Cai, Y.Q. Particle size effects on coarse soil-geogrid interface response in cyclic and post-cyclic direct shear tests. *Geotext. Geomembr.* **2016**, *44*, 854–861. [[CrossRef](#)]
22. GB/T 50123-2019; National Standards of the People’s Republic of China. Standard for Geotechnical Test Methods. Ministry of Housing and Urban-Rural Development of the People’s Republic of China: Beijing, China, 2019. (In Chinese)
23. Desai, C.S.; Drumm, E.C.; Zaman, M.M. Cyclic testing and modeling of interfaces. *J. Geotechnical. Eng.* **1985**, *111*, 793.e815. [[CrossRef](#)]
24. Nye, C.J.; Fox, P.J. Dynamic shear behavior of a needle-punched geosynthetic clay liner. *J. Geotech. Geoenvironmental Eng.* **2007**, *133*, 973–983. [[CrossRef](#)]
25. Liu, F.-y.; Wang, P.; Wang, J.; Hu, X.; Cai, Y. Experimental research on reinforcement-soil interface stiffness and damping ratio under cyclic shearing. *Rock Soil Mech.* **2016**, *37* (Suppl. S1), 159–165.

26. Liu, F.-y.; Shi, J.; Wang, J.; Cai, Y.-Q. Dynamic shear behavior of interface for clay reinforced with geogrid encapsulated in thin layers of sand. *Rock Soil Mech.* **2018**, *39*, 1991–1998.
27. Wu, M.-T.; Liu, F.-C.; Chen, J.-L.; Chen, L. Influence of water content on dynamic shear modulus and damping ratio of rubber-sand mixture under large strains. *Rock Soil Mech.* **2018**, *39*, 803–814, 847.
28. Chen, R.-F.; Yan, W.-Y.; Liu, X.-F.; Dong, X.-Q. Study of Dynamic Modulus and Damping Ratio of Loess Solidified by Red Mud under Different Water Content. *Bull. Chin. Ceram. Soc.* **2017**, *36*, 2810–2815.

Disclaimer/Publisher’s Note: The statements, opinions and data contained in all publications are solely those of the individual author(s) and contributor(s) and not of MDPI and/or the editor(s). MDPI and/or the editor(s) disclaim responsibility for any injury to people or property resulting from any ideas, methods, instructions or products referred to in the content.